Journal of Solid State Chemistry 181 (2008) 1753–1758

Contents lists available at ScienceDirect

Journal of Solid State Chemistry

journal homepage: www.elsevier.com/locate/jssc

Structural and magnetic properties of pyrochlore solid solutions $(Y,Lu)_2Ti_{2-x}(Nb,Ta)_xO_{7\pm y}$

D.V. West [a,*], T.M. McQueen [a], Q. Huang [b], R.J. Cava [a]

[a] Department of Chemistry, Princeton University, NJ 08544, USA
[b] NIST Center for Neutron Research, Gaithersburg, MD 20899, USA

ARTICLE INFO

Article history:
Received 5 December 2007
Received in revised form
19 March 2008
Accepted 24 March 2008
Available online 3 April 2008

Keywords:
Reduced niobium
Reduced titanium
Magnetism
Pyrochlore
Oxygen deficient
Oxygen excess

ABSTRACT

The synthesis and characterization of the pyrochlore solid solutions, $Y_2Ti_{2-x}Nb_xO_{7-y}$, $Lu_2Ti_{2-x}Nb_xO_{7-y}$, $Y_2Ti_{2-x}Ta_xO_{7-y}$ and Lu_2TiTaO_{7-y} ($-0.4<y<0.5$), is described. Synthesis at 1600 °C, and 10^{-5} Torr yields oxygen deficiency in all systems. All compounds are found to be paramagnetic and semiconducting, with the size of the local moments being less, in some cases substantially less, than the expected value for the number of nominally unpaired electrons present. Thermogravimetric analysis (TGA) shows that all compounds can be fully oxidized while retaining the pyrochlore structure, yielding oxygen rich pyrochlores as white powders. Powder neutron diffraction of Y_2TiNbO_7-based samples was done. Refinement of the data for oxygen deficient $Y_2TiNbO_{6.76}$ indicates the presence of a distribution of oxygen over the 8*b* and 48*f* sites. Refinement of the data for oxygen rich $Y_2TiNbO_{7.5}$ shows these sites to be completely filled, with an additional half filling of the 8*a* site. The magnetic and TGA data strongly suggest a preference for a $Ti^{3+}/(Nb,Ta)^{5+}$ combination, as opposed to $Ti^{4+}/(Nb,Ta)^{4+}$, in this pyrochlore family. In addition, the evidence clearly points to Ti^{3+} as the source of the localized moments, with no evidence for localized Nb^{4+} moments.

1. Introduction

Interest in niobium-based ceramics has stemmed primarily from the ferroelectric properties of Nb^{5+}, the fully oxidized cation, with less focus on reduced niobates having oxidation states less than 5+. Phases containing Nb^{4+} are often derivatives of the perovskite and pyrochlore structures [1], while several other, more reduced, phases possess Nb_6O_{12} clusters in which the Nb ions are found on the vertices of an octahedron [2,3]. As 4*d* valence electrons have a tendency to form Nb–Nb bonds, many reduced niobates are metals or small-band gap semiconductors. There are some claims of temperature independent paramagnetism and extremely few examples exhibiting localized magnetic moments, the most prominent of which are the block-based niobium oxide shear structures, e.g. $Nb_{12}O_{29}$ and $Nb_{22}O_{54}$ [4–6]. There have also been reports of magnetic niobate pyrochlores [7].

As a structural class, pyrochlores (general formula $A_2B_2O_6O'$) hold interest as geometrically frustrating lattices, sometimes allowing the observation of exotic phenomena, such as spin ice. A unique structure type, it has two interpenetrating frustrating *A* and *B* sub-lattices, but with different crystal field environments. Magnetic *B*-site materials such as $Y_2(Mn,Mo)_2O_7$ [8,9] have yielded insulating examples of both frustrated ferro- and antiferromagnetic materials. Meanwhile, the *A*-site materials $(Dy,Ho)_2Ti_2O_7$ have received much attention as examples of spin-ice compounds [10,11].

Recent studies on niobium-based pyrochlores, like other reduced niobates, have yielded weakly magnetic, or non-magnetic compounds. $CaLnNb_2O_7$ (Ln = Y, La, Lu) [12,13] is non-magnetic and electrically insulating, possibly explained by strong spin–orbit coupling, or electronic Nb–Nb coupling. The latter interpretation is supported by DFT calculations on $Y_2Nb_2O_7$ [14]. However, the $Ln_2Nb_2O_7$ (Ln = Y, La, Lu) phases based on Nb^{4+} cannot be synthesized under equilibrium conditions up to 1625 °C [15].

In this study, the structural and electronic properties of the solid solutions $Ln_2Ti_{2-x}M_xO_{7\pm y}$, where Ln = Y, Lu and M = Nb, Ta, are explored in order to gain a clearer understanding of the electronic and structural properties of these systems, and in particular, the magnetic attributes of niobium 4*d* electrons in the pyrochlore setting.

2. Experimental

$Y_2Ti_{2-x}Nb_xO_{7-y}$, $Lu_2Ti_{2-x}Nb_xO_{7-y}$, $Y_2Ti_{2-x}Ta_xO_{7-y}$, with $x = 0$, 0.25, 0.5, 0.75, and 1, and Lu_2TiTaO_{7-y}, were made by mixing

* Corresponding author at: Frick Laboratory, Princeton University, NJ 08544, USA. Fax: +1 609 258 6746.
E-mail addresses: barelytone@gmail.com, dwest@princeton.edu (D.V. West).

0022-4596/$ - see front matter © 2008 Elsevier Inc. All rights reserved.
doi:10.1016/j.jssc.2008.03.030

stoichiometric quantities of Y_2O_3 (Alfa Aesar, 99.999%), Lu_2O_3 (Alfa Aesar 99.9%), NbO_2 (Alfa Aesar 99+%), Nb_2O_5 (Aldrich 99.5%), Ta_2O_5 (Alfa Aesar 99.993%), and TiO_2 (Alfa Aesar 99.9%). They were then ground to homogeneity and wrapped in Nb foil. Unless otherwise specified, the samples were heated twice at 1600 °C for 12 h in a vacuum furnace under a dynamic vacuum of 10^{-5} Torr with intermittent grinding. $Y_2Ti_2O_7$ was prepared at 1500 °C in air, followed by annealing at 1500 °C under vacuum. Powder samples, as opposed to pellets, were preferred for reproducible oxygen loss caused by the high vacuum. Oxygen rich pyrochlores were produced by annealing the oxygen deficient powders at either 280 or 500 °C under flowing O_2. $CaYNb_2O_7$ was prepared as a control by mixing $Ca_4Nb_2O_9$ (prepared in air at 1300 °C from $CaCO_3$ (Mallinckrodt, 99.9%) and Nb_2O_5), Nb_2O_5, NbO_2 and Y_2O_3 stoichiometrically. The powder was pressed into a pellet, wrapped in Mo foil, and heated in a vacuum furnace back-filled with argon at 1525 °C for 32 h, with an intermediate grinding, re-pelleting and then re-heating at 1625 °C for 12 h.

Magnetic susceptibilities were measured using a Quantum Design PPMS magnetometer under a 1 T field in the temperature range 5–60 K. Susceptibility data were fit to the Curie–Weiss law in order to obtain the p_{eff} values of the samples.

Oxygen stoichiometries were determined using a TA Instruments Thermogravimetric Analyzer (TGA). Samples sizes of 20–45 mg were placed on a platinum weighing pan and heated from room temperature to 550 or 700 °C at either 0.25 or 2 °C/min under flowing O_2. Under these conditions all mass change was due to oxygen absorption, and the final mass for the white samples obtained corresponded to a state of maximal oxidation. This allowed the determination of the initial oxygen stoichiometry of the samples synthesized under high vacuum.

The $Ti^{3+/4+}$ and $Nb^{4+/5+}$ or $Ta^{4+/5+}$ ratios for all samples were estimated from the TGA curves. In all but one of the Nb-based samples, and in the Ta-based samples where $x = 1.0$ and 0.75, an intermediate region in between two mass gain transitions was observed. For these samples, linear fits to portions of the first derivatives were used to demarcate the extrema of the intermediate region. Assuming that complete oxidation of Ti^{3+} occurs before any oxidation of Nb^{4+} or Ta^{4+}, the oxygen content at which Ti^{3+} oxidation ends and Nb^{4+} or Ta^{4+} oxidation begins was approximated as half of the difference between the oxygen contents at the extrema, thus allowing an estimation of the cation oxidation state distributions in the reduced materials. For $Y_2Ti_{1.75}Nb_{0.25}O_{6.85}$ and the other Ta-based samples, no intermediate region was observed and by comparison to the other TGA plots and their trends, it is reasonable to assume that all Nb or Ta is 5+ in these samples.

Crystal structures were characterized using both X-ray and neutron diffraction of polycrystalline samples at room temperature. Powder X-ray diffraction (PXRD) data were collected with a Bruker D8-Focus, using Cu$K\alpha$ radiation with a graphite diffracted beam monochromator. Powder neutron diffraction (PND) data were collected on $Y_2TiNbO_{6.76}$ and $Y_2TiNbO_{7.5}$ at the NIST Center for Neutron Research on the high-resolution powder neutron diffractometer (BT-1) with neutrons of wavelength 1.5403 Å produced by using a Cu(311) monochromator. Collimators with horizontal divergences of 15′, 20′ and 7′ of arc were used before and after the monochromator and after the sample, respectively. Data were collected in the 2θ range of 3–168° with a step size of 0.05°. The structural parameters were determined by Rietveld refinement of the neutron diffraction data using the GSAS program [16,17]. The atomic neutron scattering factors used in the refinements were Y—0.775, Ti—(−0.337), Nb—0.705, and O—0.581×10^{-12} cm.

3. Results and discussion

One known and three new single phase pyrochlore solid solutions of the general formula $Ln_2Ti_{2-x}M_xO_{7+y}$ (Ln = Y,Lu; M = Nb,Ta; $0 \leqslant x \leqslant 1$; $-0.4 \leqslant y \leqslant 0.5$) were synthesized under high vacuum as described. Under these conditions, significant loss of oxygen occurs, yielding black powders containing a mix of $Ti^{3+/4+}$ and either $Nb^{4+/5+}$ or $Ta^{4+/5+}$. For all samples, a 500 °C anneal under flowing O_2 turns the powders white, oxidizing all of the reduced cations to Ti^{4+}, Nb^{5+} and Ta^{5+}. All of the powder diffraction patterns (Fig. 1) show the same pyrochlore peaks consistent with $Fd-3m$ symmetry. Increased doping on the Ti site with Nb or Ta systematically increases the unit cell parameter. Interestingly, the unit cell parameter increases with excess oxygen when M = Nb, but decreases when M = Ta. Since the unit cell parameter is a competition between decreasing cation size with increasing oxidation state, disruption of metal–metal bonds (if present) and extra oxygen atoms trying to occupy the same space, it is not possible to unambiguously identify the origin of the difference between the Nb and Ta cases.

The compounds $Y_2Ti_{2-x}Nb_xO_{7-y}$, $Lu_2Ti_{2-x}Nb_xO_{7-y}$, $Y_2Ti_{2-x}Ta_xO_{7-y}$ and $CaYNb_2O_7$ were measured both for their magnetic properties and their mass gain in the TGA under flowing oxygen. The measured mass gain was dependent upon the number of heatings under high vacuum with intermittent grinding, but was independent of the duration of these heatings beyond 12 h.

The TGA data for the control samples containing only Ti ($Y_2Ti_2O_{6.88}$ and $Lu_2Ti_2O_{6.64}$) or only Nb ($CaYNb_2O_7$) are shown in Fig. 2a. The titanate samples show only one mass gain around 200 °C and both show sizable effective magnetic moments per formula unit (p_{eff}/f.u.) (0.29 ± 0.01 and 0.57 ± 0.01 μ_B respectively). The niobate also shows only one transition, but at 400 °C, and the compound is non-magnetic.

Y_2TiNbO_{7-y} was made by heating the sample four times under high vacuum with intermittent grindings. After each heating, some of the powder was measured for oxygen gain in the TGA on heating in O_2 (Fig. 2b). In all cases, the curves show the same general shape: two mass increases, one just above 200 °C and another just above 400 °C, surrounding an intermediate region with a substantially smaller slope. The control samples indicate that the low temperature mass increase is associated with

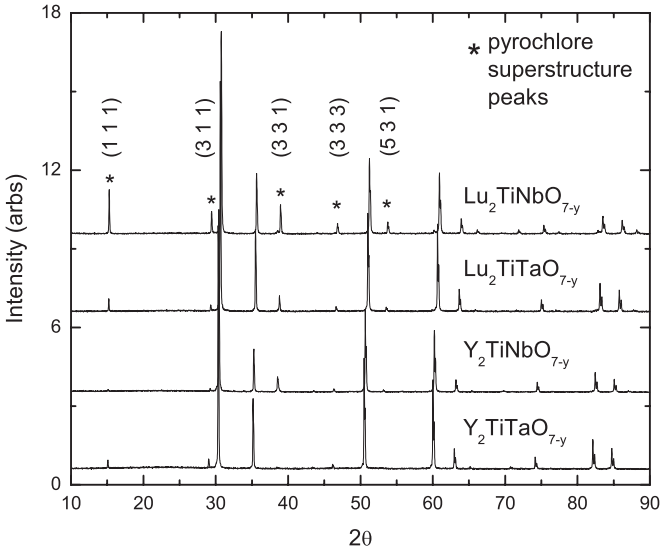

Fig. 1. XRD patterns of the $x = 1$ samples from each of the four solid solutions in order from smallest (top) to largest (bottom) unit cell parameters. Pyrochlore superstructure peaks are indicated by the arrows, with corresponding Miller indices.

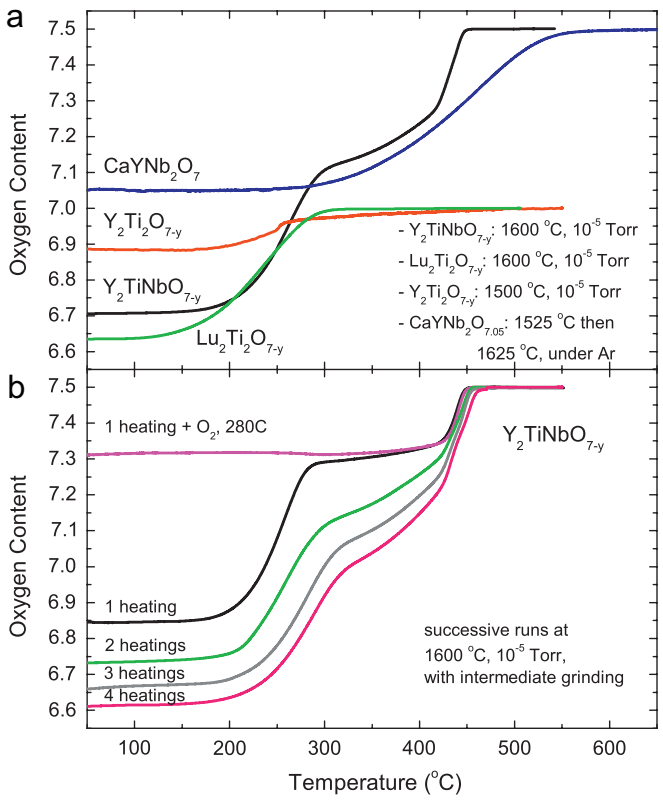

Fig. 2. (a) TGA data for Y_2TiNbO_{7-y} showing that with repeated heating, the second transition, corresponding to Nb^{4+} oxidation, grows larger while the first transition, corresponding to Ti^{3+} oxidation, remains unchanged. (b) Comparison of the oxidation of Y_2TiNbO_{7-y} to Ti-only compounds ($(Y,Lu)_2Ti_2O_{7-y}$) and an Nb-only compound ($CaYNb_2O_{7-y}$) showing the first and second transitions to be the oxidation of Ti^{3+} and Nb^{4+} respectively.

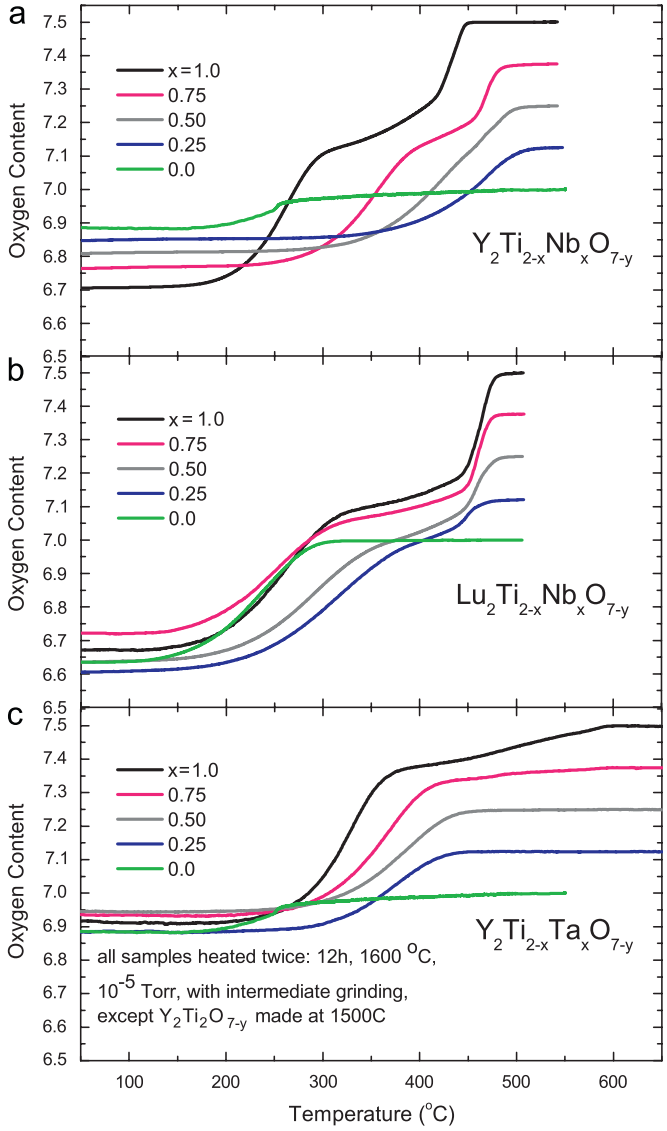

Fig. 3. TGA data for (a) $Y_2Ti_{2-x}Nb_xO_{7-y}$, (b) $Lu_2Ti_{2-x}Nb_xO_{7-y}$ and (c) $Y_2Ti_{2-x}Ta_xO_{7-y}$. A comparison of the two niobium compounds clearly shows the second transition gets smaller with decreasing Nb content. By contrast, the Ta compounds show very little in the second transition indicating the significant preference for Ta^{5+} over Ta^{4+}.

oxidation of Ti^{3+}, and the high temperature increase with oxidation of Nb^{4+}. The exact nature of the intermediate region, whose slope changes gradually with increased amounts of heating, is unknown. Some of the sample from the first heating was annealed overnight under flowing O_2 gas at 280 °C. The annealed sample was found to be non-magnetic. Subsequent analysis in the TGA shows that the annealed sample has one mass gain just after 400 °C, equal in magnitude to the second transition seen in its parent sample. This indicates that all of the magnetic electrons are associated with the low temperature oxidation, thus pointing to Ti^{3+}, and not Nb^{4+}, as the source of localized magnetism. Two of the other samples, the ones heated twice and four times with intermediate grindings, were measured in the magnetometer as well. They were found to have the same p_{eff}/f.u. within error ($0.33 \pm 0.01\ \mu_B$), in spite of having significantly different oxygen contents.

For the series $Y_2Ti_{2-x}Nb_xO_{7-y}$, as x decreases fewer oxygen vacancies are created by the high-vacuum heatings (Fig. 3a), with the full titanate sample having the formula $Y_2Ti_2O_{6.88}$. As x decreases, the temperature range of the intermediate region grows smaller, disappearing entirely by the $x = 0.25$ sample. These TGA data show that the oxidation states of the *B*-site cations exist as a mixture of $Ti^{3+/4+}$ and $Nb^{4+/5+}$, with the oxidation of the reduced cations happening at separate temperatures in spite of being randomly mixed. The magnetic data for this family is shown in Fig. 4a. The size of p_{eff}/f.u. for all of these samples was small and changed little across the series (Fig. 5).

The $Lu_2Ti_{2-x}Nb_xO_{7-y}$ series (Fig. 3b) contrasts to the Y analogue in several ways. In this series, the temperature range of the intermediate region shrinks as before, but is clearly seen in all niobium-containing samples. And while the titanate end-member retains a single mass gain at 200 °C, the oxygen content is significantly lower than its Y counterpart at $Lu_2Ti_2O_{6.64}$, possibly due to the smaller size of Lu^{3+}, which is expected to allow it to accommodate fewer oxygen neighbors. Like its Y analogue, the *B*-site cations in these compounds possess a $Ti^{3+/4+}$–$Nb^{4+/5+}$ mixture of oxidation states. Across the series, the magnetic moment was its lowest at $x = 1.0$ (p_{eff}/f.u. $= 0.28 \pm 0.01\ \mu_B$), about the same at $x = 0.75$, and then rose steadily to its highest moment at $x = 0$ ($0.57 \pm 0.01\ \mu_B$), significantly larger than the Y analogue (see Figs. 4 and 5).

$Y_2Ti_{2-x}Ta_xO_{7-y}$ shows markedly different behavior (Fig. 3c) reflecting the influence of the more electropositive Ta in place of Nb. Examining first the $x = 1.0$ compound, the TGA curve corresponds to an initial stoichiometry of $Y_2TiTaO_{6.9}$, implying a 20% reduction of the Ta^{5+} to Ta^{4+}. The same initial mass gain at 200 °C is seen followed by a very gradual and small mass gain up to 600 °C, presumed to be Ta^{4+} oxidation. Because it occurs at

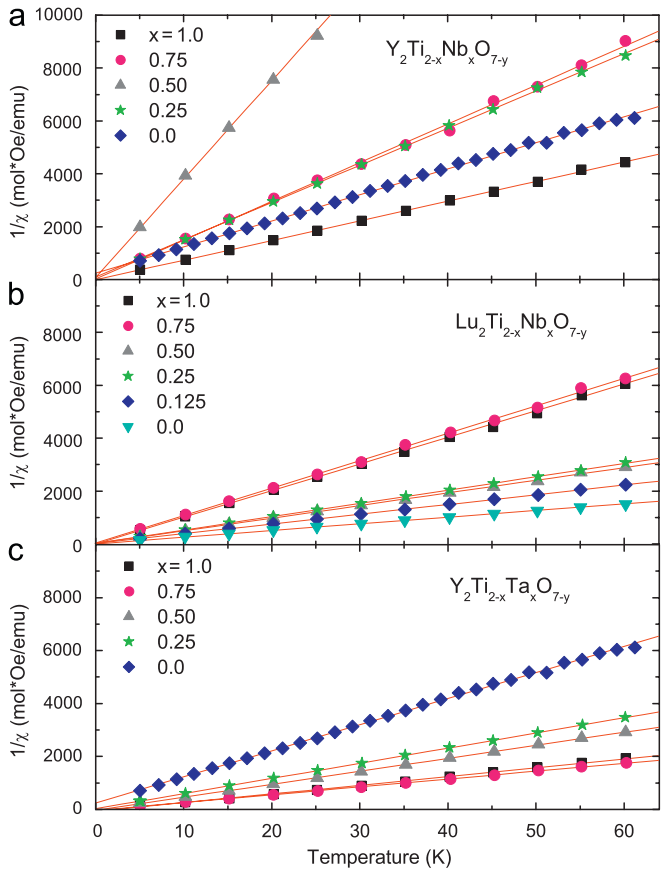

Fig. 4. $1/\chi$ vs. T plots for (a) $Y_2Ti_{2-x}Nb_xO_{7-y}$, (b) $Lu_2Ti_{2-x}Nb_xO_{7-y}$ and (c) $Y_2Ti_{2-x}Ta_xO_{7y}$. All samples were heated twice at 1600 °C under high vacuum. All samples show Curie Weiss behavior down to 5 K, with small Curie constants and negligible values of θ_w.

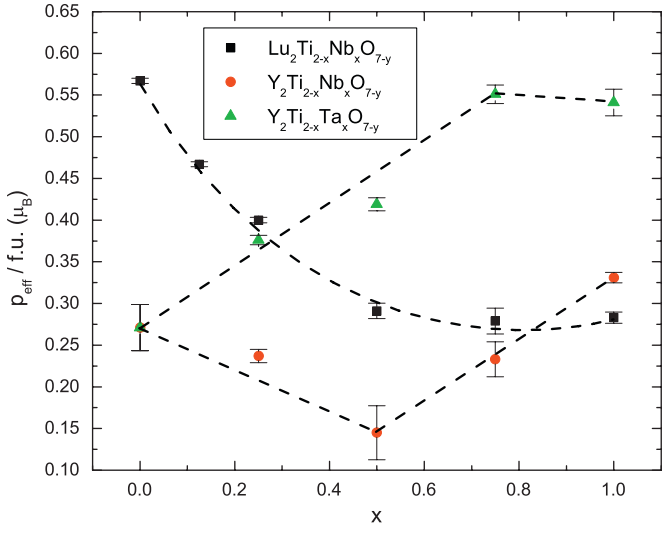

Fig. 5. Comparison of the p_{eff}/f.u. (effective magnetic moment per formula unit) as a function of x for three of the solid solutions. The comparison of the Y and Lu series based on Ti/Nb reflect the lower tolerance of oxygen deficiency in the Y case, possibly owing to its bigger size. The lines are drawn to guide the eye.

higher temperature than the initial mass gain, the oxidation of Ti^{2+} to Ti^{3+} in the parent material is an unlikely explanation of the second mass gain because Ti^{2+} oxidation would have to occur before the Ti^{3+} oxidation. The $x = 0.75$ sample retains a small amount of this high temperature gradual mass gain, but for $x < 0.75$, only the low temperature transition is observed. The magnetic susceptibility data are shown in Fig. 4c. Across the series, the p_{eff}/f.u was its highest at $x = 1.0$ (0.54 μ_B), about the same at $x = 0.75$, and decreased steadily to its lowest at $x = 0$ (0.26 μ_B) (Fig. 5). Tantalum has never been shown to exhibit localized magnetism, and as such these data clearly indicate Ti^{3+} as the source of the local moments for this series.

Comparing all three series, it is useful to plot the p_{eff}/f.u. vs. Ti^{3+}/f.u or Nb^{4+}/f.u. (Table 1, Fig. 6). The correlations of the p_{eff}/f.u. to the Ti^{3+}/Nb^{4+} contents were quite different between the three series. For the Nb-based compounds, it is very difficult to draw any correlation between Ti^{3+} content and p_{eff}. For the series $Y_2Ti_{2-x}Nb_xO_{7-y}$, the local moment changes little even as the Ti^{3+} content varies significantly. Conversely, the Lu analogue has fairly constant Ti^{3+} content, but displays a changing local moment. Looking instead at Nb^{4+} content, there is no discernible trend in the Y-based series, but for the Lu-based series the local moment decreases as Nb^{4+} content increases (Fig. 6a). Compared to the Nb-based compounds, $Y_2Ti_{2-x}Ta_xO_{7-y}$ exhibits a more rational trend (Fig. 6b), with the local moment increasing steadily with increasing Ti^{3+} content. Also, the Ti-only compound $Lu_2Ti_2O_{6.64}$ sits close to the trend formed by the $Y_2Ti_{2-x}Ta_xO_{7-y}$ series in the p_{eff} vs. Ti^{3+} plot (Fig. 6b), further stressing the relationship of the magnetism to localized Ti^{3+} states.

A DFT study on $Y_2Nb_2O_7$ by Blaha et al. [14], supported by structural studies done in our lab on Nb-based pyrochlores (including Y_2TiNbO_7), indicate that a *B*-site displacement, in which Nb^{4+} atoms move off the 16*c* sites toward the center of the *B*-sublattice tetrahedra forming a 4-center 2-electron bond, is prevalent in Nb^{4+} pyrochlores [15]. Though not conclusive, the data presented here are consistent with these observations, and suggest that niobium may be suppressing magnetism by replacing the paramagnetic states with singlet states, while the tantalum is a spectator ion.

$Y_2TiNbO_{6.76}$ and $Y_2TiNbO_{7.5}$ were studied by PND (Fig. 7). The data were refined using two models: the standard pyrochlore model, and a *B*-site displacement model (Table 2). We refined this second model to compare these samples to the DFT calculations and the other work in our lab [15]. The *B* cations occupy the vertices of perfect tetrahedra that share corners infinitely in all directions. As each *B* atom is shared by two tetrahedra, the

Table 1
Correlation of the effective moment to the reduced cation concentrations determined by TGA

	μ_B/f.u.	mol Ti^{3+}/f.u.	mol Nb^{4+}/f.u.
$Y_2Ti_{2-x}Nb_xO_{7-y}$			
$x = 1.00$	0.33(1)	0.98	0.61
$x = 0.75$	0.23(2)	0.81	0.41
$x = 0.50$	0.15(3)	0.66	0.22
$x = 0.25$	0.24(1)	0.56	0
$x = 0.00$	0.27(3)	0.24	–
$Lu_2Ti_{2-x}Nb_xO_{7-y}$			
$x = 1.00$	0.28(1)	0.94	0.72
$x = 0.75$	0.28(2)	0.79	0.50
$x = 0.50$	0.29(1)	0.81	0.42
$x = 0.25$	0.400(3)	0.81	0.26
$x = 0.00$	0.567(3)	0.73	–
$Y_2Ti_{2-x}Ta_xO_{7-y}$			mol Ta^{4+}/f.u.
$x = 1.00$	0.54(1)	0.94	0.23
$x = 0.75$	0.55(1)	0.81	0.07
$x = 0.50$	0.42(1)	0.62	0
$x = 0.25$	0.38(1)	0.49	0
$x = 0.00$	0.27(3)	0.24	–

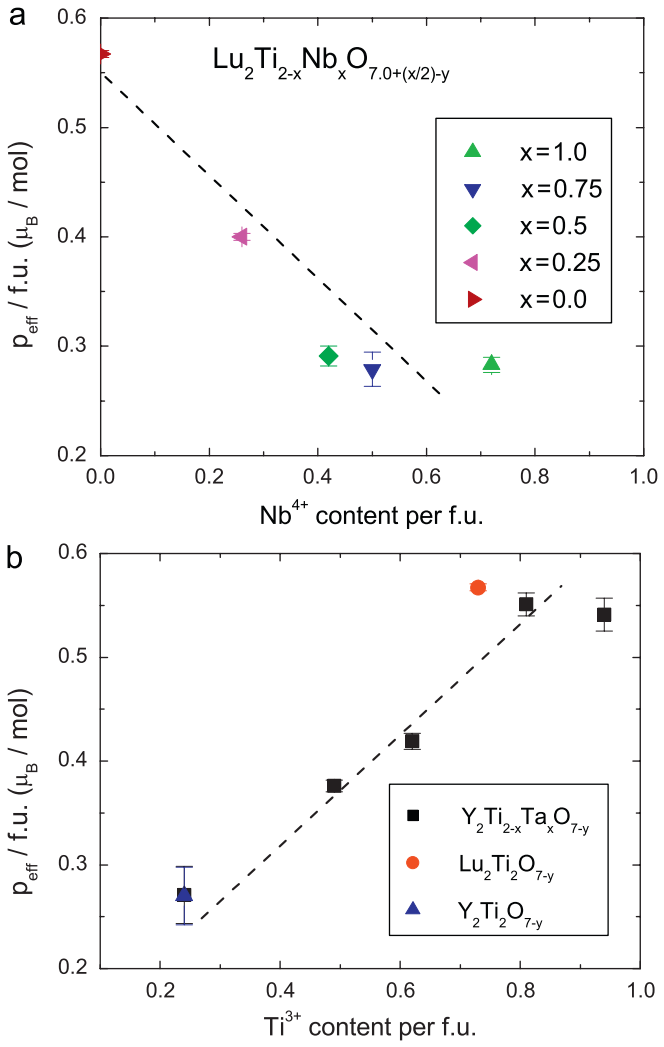

Fig. 6. (a) Plot showing the negative correlation of p_{eff}/f.u. to the amount of Nb^{4+} in the series $Lu_2Ti_{2-x}Nb_xO_{7-y}$, estimated from the TGA data. (b) Plot showing the positive correlation of p_{eff}/f.u. to the amount of Ti^{3+} for all the compounds measured that do not contain Nb. The lines are drawn to guide the eye.

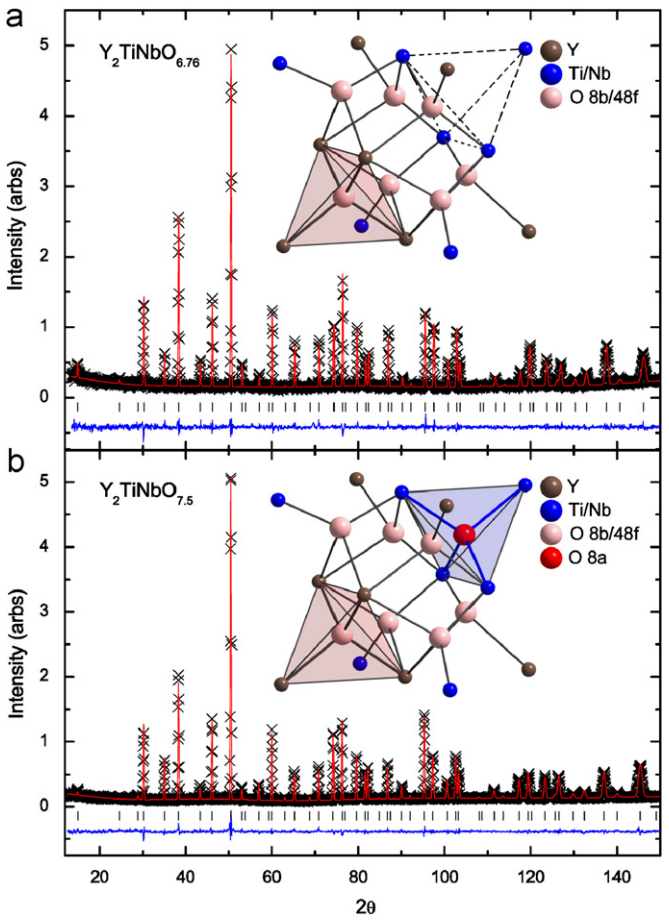

Fig. 7. (a) Neutron diffraction data for oxygen deficient Y_2TiNbO_{7-y}, refined with *Fd*−3*m* symmetry. Refinement of the oxygen occupancies shows a distribution of oxygen on the 8*b* and 48*f* sites. Inset: 1/8 of the unit cell showing the distributed 8*b* and 48*f* oxygens, and the 8*a* oxygen sitting in the Y tetrahedron, and the empty Ti/Nb tetrahedron. (b) Neutron diffraction data for oxygen rich Y_2TiNbO_{7-y}, refined with *Fd*−3*m* symmetry and 0.5 occupancy on the 8*a* site. Inset: 1/8 of the unit cell showing the 1/2 occupied 8*a* site, sitting within the Ti/Nb tetrahedron.

displacement moves them closer to the center of one tetrahedron, and farther away from the other. In both cases, it was found that the temperature factors for the *B*-site cations and χ^2 values were reduced for the displaced atom model. In both cases the displacement was statistically significant, though slightly smaller in the oxygen rich case. This refinement leaves open the possibility that the non-systematic magnetic trends in the Nb-based compounds are explained by the formation of singlet states.

For the oxygen deficient sample, the oxygen occupancies were refined while constrained to sum to the value determined by TGA. For the oxygen rich sample, the excess oxygen was placed on the 8*a* site (pyrochlores are defect fluorite structures, which have one out of eight anion sites vacant; this vacancy corresponds to the 8*a* site, and is the only possible site for excess oxygen to go). While constraining them to sum to the oxygen content corresponding to the state of maximal oxidation, refining the oxygen occupancies resulted in greater than unit occupancies on either the 8*b* or the 48*f* sites, and less than half occupancy on the 8*a* site. As there is no other rational site for the oxygens in the pyrochlore structure, the 8*b* and 48*f* oxygen occupancies were constrained to one, with half occupancy on the 8*a* site. We note that there is no thermodynamically stable phase $Y_2TiNbO_{7.5}$. The equilibrium assemblage for samples synthesized at 1600 °C with this formula is $Y_2Ti_2O_7$ and $YNbO_4$.

4. Conclusion

One known, and three new pyrochlore solid solutions, have been synthesized and characterized. PND studies show a distribution of the oxygen between the 8*b* and 48*f* sites for $Y_2TiNbO_{6.76}$, and a half occupancy of the 8*a* site for $Y_2TiNbO_{7.5}$. In addition, the data for this Nb-based compound are consistent with both a standard pyrochlore model, and a *B*-site displacement model in which the *B*-site cations displace off of their special positions.

TGA and magnetic studies suggest some preference for a Ti^{3+}/M^{5+} combination in these solid solutions, rather than a purely Ti^{4+}/M^{4+} combination on the *B*-site. Moreover, the loss of magnetism after the low temperature oxidation, shown to be Ti^{3+} oxidation, indicates Ti^{3+} as the source of local moments in these compounds. This conclusion is further supported by the increase in the p_{eff}/f.u. with the increase in Ti^{3+} content for the Ti-only and Ti/Ta-based compounds. These results indicate that the pyrochlore family of niobates, unlike the crystallographic shear structures, does not support the existence of local moment magnetism for Nb^{4+}.

Table 2
Structural parameters from powder neutron diffraction *Fd*-3*m*, 8*a* ($\frac{1}{8},\frac{1}{8},\frac{1}{8}$); 8*b* ($\frac{3}{8},\frac{3}{8},\frac{3}{8}$); 16*c* (0,0,0); 16*d* ($\frac{1}{2},\frac{1}{2},\frac{1}{2}$); 32*e* (*x*, *x*, *x*); 48*f* ($x,\frac{1}{8},\frac{1}{8}$)

	$Y_2TiNbO_{6.76}$		$Y_2TiNbO_{7.5}$	
	Normal	Displaced model	Normal	Displaced model
Y				
Site	16*d*	16*d*	16*d*	16*d*
Occ	1	1	1	1
B_{iso}	0.87(3)	0.88(3)	0.86(2)	0.87(2)
Ti/Nb				
Site	16*c*/16*c*	32*e*/32*e*	16*c*/16*c*	32*e*/32*e*
x	0	0.013(1)/0.013(1)	0	0.007(1)/0.007(1)
Occ	0.5/0.5	0.25/0.25	0.5/0.5	0.25/0.25
B_{iso}	3.5(2)/3.5(2)	2.1(3)/2.1(3)	1.7(1)/1.7(1)	1.3(2)/1.3(2)
O1				
Site	8*b*	8*b*	8*b*	8*b*
Occ	0.98(2)	0.98(2)	1	1
B_{iso}	0.69(10)	0.59(10)	0.72(4)	0.70(4)
O2				
Site	48*f*	48*f*	48*f*	48*f*
x	0.3350(1)	0.3347(2)	0.3354(1)	0.3353(1)
Occ	0.966(3)	0.964(3)	1	1
B_{11}	1.40(6)	1.47(6)	2.91(5)	2.96(5)
$B_{22}=B_{33}$	0.78(3)	0.82(4)	0.82(2)	0.85(2)
O3				
Site	–	–	8*a*	8*a*
Occ	–	–	0.5	0.5
B_{iso}	–	–	2.5(1)	2.4(1)
a (Å)	10.1805(1)	–	10.2015(1)	–
χ^2	0.9836	0.9759	1.051	1.045
R_p (%)	7.02	6.98	5.91	5.88
R_{wp} (%)	8.99	8.96	7.38	7.37

Acknowledgments

This research was supported by the NSF program in Soild State Chemistry, Grant number NSF DMR-0703095. Certain commercial materials and equipment are identified in this report to describe the subject adequately. Such identification does not imply recommendation or endorsement by the NIST, nor does it imply that the materials and equipment identified are necessarily the best available for the purpose. T.M. McQueen gratefully acknowledges support of the National Science Foundation Graduate Research Fellowship Program.

References

[1] O.G. D'yachenko, S.Y. Istomin, A.M. Abakumov, E.V. Antipov, Inorg. Mater. 36 (2000) 247–259.
[2] B. Hessen, S.A. Sunshine, T. Siegrist, A.T. Fiory, J.V. Waszczak, Chem. Mater. 3 (1991) 528–534.
[3] J. Kohler, G. Svensson, A. Simon, Angew. Chem. Int. Ed. 31 (1992) 1437–1456.
[4] R.J. Cava, B. Batlogg, J.J. Krajewski, P. Gammel, H.F. Poulsen, W.F. Peck, L.W. Rupp, Nature 350 (1991) 598–600.
[5] J.E.L. Waldron, M.A. Green, D.A. Neumann, J. Am. Chem. Soc. 123 (2001) 5833–5834.
[6] T. McQueen, Q. Xu, E. Andersen, H.W. Zandbergen, R.J. Cava, J. Solid State Chem. 180 (2007) 2864–2870.
[7] O. Sakai, Y. Jana, R. Higashinaka, H. Fukazawa, S. Nakatsuji, Y. Maeno, J. Phys. Soc. Japan 73 (2004) 2829–2833.
[8] J.E. Greedan, M. Sato, Y. Xu, F.S. Razavi, Solid State Commun. 59 (1986) 895–897.
[9] J.N. Reimers, J.E. Greedan, R.K. Kremer, E. Gmelin, M.A. Subramanian, Phys. Rev. B43 (1991) 3387–3394.
[10] M.J. Harris, S.T. Bramwell, D.F. McMorrow, T. Zeiske, K.W. Godfrey, Phys. Rev. Lett. 79 (1997) 2554–2557.
[11] A.P. Ramirez, A. Hayashi, R.J. Cava, R. Siddharthan, B.S. Shastry, Nature 399 (1999) 333–335.
[12] S.Y. Istomin, O.G. D'Yachenko, E.V. Antipov, G. Svensson, Mater. Res. Bull. 32 (1997) 421–430.
[13] S.Y. Istomin, O.G. D'Yachenko, E.V. Antipov, G. Svensson, B. Lundqvist, Mater. Res. Bull. 33 (1998) 1251–1256.
[14] P. Blaha, D.J. Singh, K. Schwarz, Phys. Rev. Lett. 93 (2004) 216403.
[15] T.M. McQueen, D.V. West, B. Muegge, Q. Huang, K. Noble, H.W. Zandbergen, R.J. Cava, J. Phys.: Condens. Matter 2008, submitted for publication. arXiv:0804.1900.
[16] A.C. Larson, R.B. Von Dreele, Los Alamos National Laboratory Report LAUR, 2000, pp. 86–748.
[17] B.H. Toby, J. Appl. Crystallogr. 34 (2001) 210–213.